Journal of Statistical Physics, Vol. 45, Nos. 3/4, 1986

Collapse of Two-Dimensional Linear Polymers

H. Saleur[1]

Received January 28, 1986

We study the collapse transition of a two-dimensional, very long polymer. The model we consider is a lattice model where the chain is represented by a self-avoiding walk with nearest-neighbor attraction. By using the transfer matrix technique we calculate exactly the thermal and geometrical properties of the polymer on strips of finite width. We then use finite-size scaling to determine the values of the tricritical (θ point) exponents

$$\nu_t = 0.55 \pm 0.01$$

$$\nu_u = 1.15 \pm 0.15$$

$$\frac{\gamma_t}{\nu_t} = 1.80 \pm 0.05$$

We compare these results to the other values already proposed in the literature.

KEY WORDS: 2D linear polymers, collapse transition, θ point, tricritical exponents.

1. INTRODUCTION

The segments of polymer chains in solution interact in a rather complex way,[1-3] the excluded volume giving rise to a repulsion while long-range Van der Waals forces produce an attraction. In the high-temperature (good solvent) regime, the repulsive interactions dominate and the chains are extended. By decreasing the temperature one can enter in the poor solvent regime where the attractive forces dominate. In this case one observes experimentally the precipitation of a polymer aggregate.[1] One can also observe the collapse of an isolated polymer chain if the solution is very

[1] Service de Physique Théorique, CEA-Saclay, 91191 Gif-sur-Yvette Cedex, France.

0022-4715/86/1100-0419$05.00/0

dilute.[4] The study of this transition has been the subject of constant investigations for many years.

Demixtion curves have been systematically studied, both experimentally and theoretically, by means of Flory Huggins approximations.[1] The collapse of a single-polymer chain has been investigated by enumerations on lattice models,[5] Monte Carlo simulations,[6] and different mean field type theories[7-10] with rather controversial results.[7,8] A systematic approach has been proposed by de Gennes[11] who related the collapse transition to the tricritical point of a magnetic spin model with zero component. With this analogy one predicts various scaling behaviors for the properties of an isolated polymer chain, which have been verified in Monte Carlo simulations.[12] The logarithmic corrections, which are present because the dimension $D = 3$ is the upper critical dimension of the problem, have been calculated by field theory methods[13] or direct polymer approaches.[14] Some tricritical properties of the demixtion curves have also been studied by these methods.[13]

The collapse transition in the two-dimensional case that can also be observed experimentally[15] is a subject of more recent interest.[16,17] In this work we study this problem by doing transfer matrix calculations on a lattice model and then using finitesize scaling. Our approach is very similar to the one which was used to study the collapse of branched polymers in Ref. [18]. Some preliminary results have been published elsewhere.[19]

The model we consider is the usual lattice model[5,17] where the polymers are represented by nonintersecting, selfavoiding walks (SAWs) on a regular twodimensional lattice (we generally present our results in the case of the square lattice). An energy $-b(\mathscr{C})$ is associated to each configuration $\mathscr{C}$ where $b(\mathscr{C})$ is the number of pairs of neighboring occupied sites not adjacent on a chain. This energy represents the attractive forces between monomers while the excluded volume effects are taken into account by the selfavoiding constraint. This model is generally believed to contain the essential features of the collapse transition.

In the following we restrict ourselves to the study of the properties of one single very long polymer.

The partition function of a polymer of l links and a fixed origin is given at a temperature $T(\beta = T^{-1})$ by

$$z_l(T) = \sum_{\mathscr{C}} e^{\beta b(\mathscr{C})} = \sum_b w(l, b)\, e^{\beta b} \tag{1}$$

where $w(l, b)$ is the number of configurations of a SAW with fixed origin of length l and energy $-b$. In the thermodynamic limit $(l \mapsto \infty)$ this partition function behaves asymptotically like

$$z_l(T) \sim [\mu(T)]^l \tag{2}$$

(when $T=\infty$, μ is the connectivity constant of the lattice). The free energy per monomer of a very long polymer with fixed origin is thus simply given by

$$f(T) = -T \lim_{l \to \infty} \frac{1}{l} \log z_l(T) = -T \log \mu(T) \tag{3}$$

All the thermodynamic quantities of interest (energy, entropy, specific heat) can be obtained from the knowledge of f. We see that these quantities display a singularity at a certain temperature θ.

In a polymer problem one is also interested in geometrical quantities. The most important geometrical property of a polymer is its mean square, end to end distance

$$\langle |\vec{R}_l|^2 \rangle = \sum_{\mathscr{C}} |\vec{R}_l(\mathscr{C})|^2 e^{\beta b(\mathscr{C})} / \sum_{\mathscr{C}} e^{\beta b(\mathscr{C})} = \sum_{\vec{R}} |\vec{R}|^2 \sum_b w_{o\vec{R}}(l, b)\, e^{\beta b}/z_l \tag{4}$$

where $\vec{R}_l(\mathscr{C})$ is the end to end distance of a polymer of length l in the configuration $\mathscr{C}$ and $w_{o\vec{R}}(l, b)$ is the number of configurations of a polymer of length l and energy $-b$ with extremities in o and $\vec{R}$. The asymptotic behavior of this mean square, end to end distance defines the exponent ν

$$\langle |\vec{R}_l|^2 \rangle \sim l^{2\nu} \tag{5}$$

At infinite temperature, the energies of the configurations play no role and the exponent ν is given by $\nu = \nu_{\mathrm{SAW}} = \frac{3}{4}$.[20] We see that this exponent jumps at the temperature θ. For $T > \theta$, one has $\nu = \nu_{\mathrm{SAW}}$ and for $T < \theta$, $\nu = 1/D = \frac{1}{2}$, the chain being collapsed. At the temperature θ, this exponent has a nontrivial value ν_t. In a polymer problem one can also introduce the exponent γ, which describes the corrections to (2) by

$$z_l(T) \sim [\mu(T)]^l\, l^{\gamma - 1} \tag{6}$$

This exponent intervenes in particular in the correlation function between the extremities of the polymer[2,3] As in the case of the exponent ν one has $\gamma = \gamma_{\mathrm{SAW}} = 43/32$ (see Ref. 20) for $T > \theta$ while γ takes a nontrivial value γ_t for $T = \theta$. The meaning of γ in the collapsed phase $T < \theta$ is not clear to us.

At temperature T the most important thermal and geometrical properties of a single very long polymer depend thus simply on $\mu(T)$, ν and γ. These quantities can be obtained by considering the generating function[18]

$$g_{o\vec{R}}(x, T) = \sum_{l,b} x^l e^{\beta b} w_{o\vec{R}}(l, b) \tag{7}$$

One can show[2,3,21] that for $x < x^c(T) = 1/\mu(T)$ this function decreases exponentially with the distance $|\vec{R}|$ like

$$g_{o\vec{R}}(x, T) \sim \exp \frac{-|\vec{R}|}{\xi(x, T)} \tag{8}$$

This defines a correlation length $\xi(x, t)$ which diverges when $x \mapsto x^c(T)$ with exponent ν

$$\xi(x, T) \sim |x - x^c(T)|^{-\nu} \tag{9}$$

In a similar way, the function

$$G(x, T) = \sum_l x^l z_l(T) = \sum_{\vec{R}} g_{o\vec{R}}(x, T) \tag{10}$$

diverges when $x \mapsto x^c(T)$ with exponent γ

$$G(x, T) \sim |x - x^c(T)|^{-\gamma} \tag{11}$$

One sees thus that the knowledge of $g_{o\vec{R}}(x, T)$ allows the determination of the thermal and geometrical properties of a very long polymer. This function will play a central role in our calculation.

The paper is organized as follows. In Section 2 we calculate the properties of a very long polymer on strips. In Section 3 we apply the phenomenological renormalization to the determination of the critical line $x^c(T) = 1/\mu(T)$ and its exponents. We then interprete the θ point as a tricritical point with respect to the two parameters T and x and we determine its characteristics in Section 4. In the conclusion we summarize our results and discuss them.

2. THERMODYNAMIC AND GEOMETRICAL PROPERTIES OF A VERY LONG POLYMER ON STRIPS

In this section we determine the properties of a polymer on strips of width n and periodic boundary conditions in the thermodynamic limit ($l \mapsto \infty$). As explained in the introduction, these properties can be obtained from the knowledge of $g_{o\vec{R}}(x, T)$. On a strip, this function can be calculated using the transfer matrix technique. We don't describe in details the calculation here since it is a simple generalization of what has already been done for interacting animals[18] and usual SAWs.[22,23] Let us simply mention that because of the nearestneighbor attraction, the information to be keept is more important than for usual SAWs and thus the size S_n of the transfer matrix grows more rapidly with the width n of the strip. We have

seen that the behavior of $g_{o\vec{R}}$ when $|\vec{R}| \mapsto \infty$ defines a correlation length ξ. On a strip of width n it is given by

$$\xi_n(x, T) = \frac{-1}{\log \lambda(x, T)} \tag{12}$$

where λ is the largest eigenvalue of the transfer matrix. This correlation length diverges at a value $x = x_n^c(T)$, which is the smallest positive root of

$$\lambda[x_n^c(T), T] = 1 \tag{13}$$

and the free energy per monomer of a very long polymer is thus given by

$$f_n(T) = T \log x_n^c(T) \tag{14}$$

All the thermodynamic quantities can be deduced from f, i.e., from the values of $x_n^c(T)$. We consider, for example, the specific heats which can be obtained by

$$c_n(t) = -T\frac{d^2 f_n}{dT^2} = -\beta^2 \frac{d^2}{d\beta^2} \log x_n^c \tag{15}$$

We have represented on Fig. 1 these specific heats versus $\beta = T^{-1}$ in the case of the square lattice. Fig. 1(a) corresponds to strips oriented in the (1, 0) direction and Fig. 1(b) to strips oriented in the (1, 1) direction. Such diagonal strips have already been used in transfer matrix calculations.[18] For strips in the (1, 0) direction we have been limited to a width $n = 7$, in which case $S_n = 202$. For strips in the (1, 1) direction, the maximum width is $n = 6$ where $S_n = 330$.

One can see on this figure that the specific heats c_n present a maximum around $\beta \simeq 0.7$. However, this maximum is not very marked and it is not clear on these curves whether the specific heats c_n will finally diverge in the limit $n \mapsto \infty$. We come to this point later. The curves of Fig. 1 also present parity effects. This means that the results converge in a regular way with the strip width n only when one compares widths of the same parity. This is particularly marked in the case of diagonal strips (Fig. 1b). Such effects not present in the case of branched polymers[18] make the analysis of the results more difficult.

Because a strip is a one-dimensional system the exponents ν and γ have simple values $\nu = \gamma = 1$. The mean size of the polymer is proportional to its length[22]

$$\langle |\vec{R}_l| \rangle = l \left\{ \frac{\partial \log \lambda[x_n^c(T), T]}{\partial \log x} \right\}^{-1} \tag{16}$$

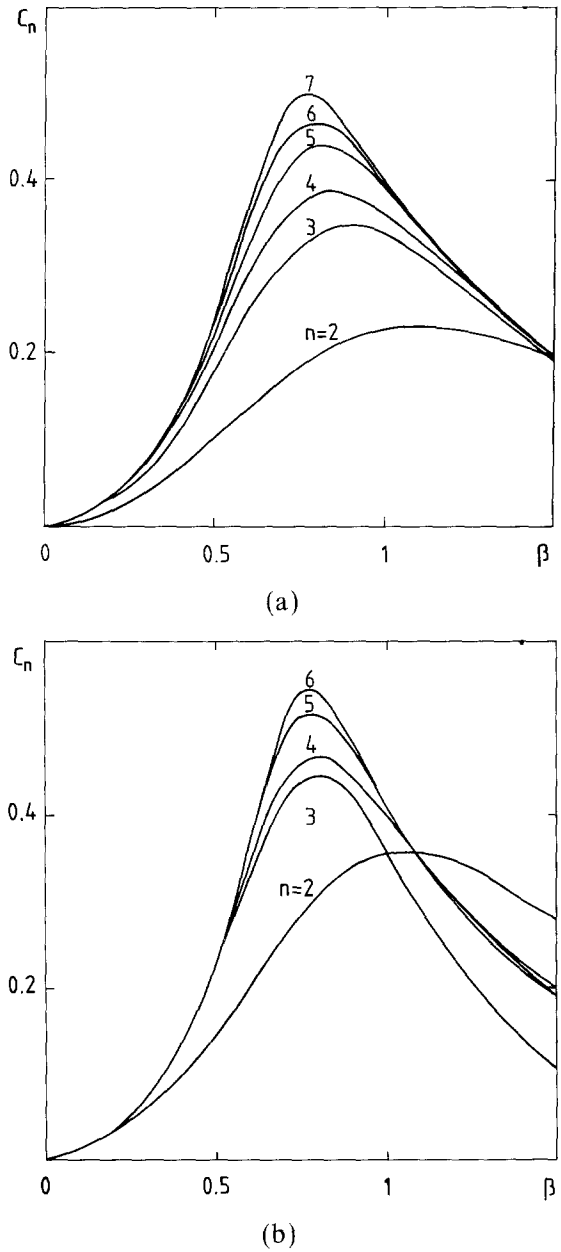

Fig. 1. Plot of the specific heat per monomer of a very long polymer c_n versus the inverse temperature $\beta = T^{-1}$ for different strip widths. (a) Strips in normal (1, 0) direction, (b) strips in diagonal (1, 1) direction. The lattice is the square lattice.

and the constant of proportionality gives the density of a very long polymer on the strip[18,19]

$$\rho_n(T) = \frac{1}{n} \frac{\partial \log \lambda[x_n^c(T), T]}{\partial \log x} \tag{17}$$

We give in Fig. 2 the curves representing ρ_n versus $\beta = T^{-1}$ in the case of the square lattice and strips oriented in normal or diagonal direction. In the small β (high-temperature) region, the densities decrease regularly with the strip width n, suggesting that the polymer is extended. On the contrary, for $\beta \gtrsim 0.7$, these densities saturate to a finite value. This suggests that the polymer is collapsed for low temperatures.

We finally introduce the coefficient of thermal expansion

$$t_n = -\frac{1}{\rho_n} \frac{d\rho_n}{dT} \tag{18}$$

We have represented this coefficient versus $\beta = T^{-1}$ in Fig. 3. The curves present a sharp maximum around the value $\beta \simeq 0.7$ corresponding to the apparition of a finite polymer density in Fig. 2. This maximum is particularly marked in the case of diagonal strips.

These results suggest thus that the properties of a very long polymer have a singularity at a temperature $\theta \sim 0.7^{-1} \sim 1.4$, the low-temperature region corresponding to a collapsed phase. We complete the study of these properties by using the phenomenological renormalization.

3. STUDY OF THE CRITICAL LINE USING THE PHENOMENOLOGICAL RENORMALIZATION

We have seen in the Introduction how the function $g_{o\bar{R}}(x, T)$ defines a correlation length which diverges as $x \mapsto x^c(T)$ with the exponent ν. When $T = \infty$ this corresponds to the second-order phase transition of the magnetic spin model with zero component[2,21] which has already been studied using the phenomenological renormalization in Ref. [23]. We apply here the same method to the case $T \neq \infty$. We suppose that the correlation length (12) ξ_n at fixed T has the following finite-size scaling form[24]

$$\xi_n(x, T) \sim n F_\xi\{[x - x^c(T)]\, n^{1/\nu}\} \tag{19}$$

for $n \gg 1$ and $x - x^c \ll 1$. Successive estimates $\tilde{x}_n^c(T)$ of $x^c(T)$ can thus be obtained by solving the equations

$$\frac{\xi_n(\tilde{x}_n^c, T)}{n} = \frac{\xi_{n+2}(\tilde{x}_n^c, T)}{n+2} \tag{20}$$

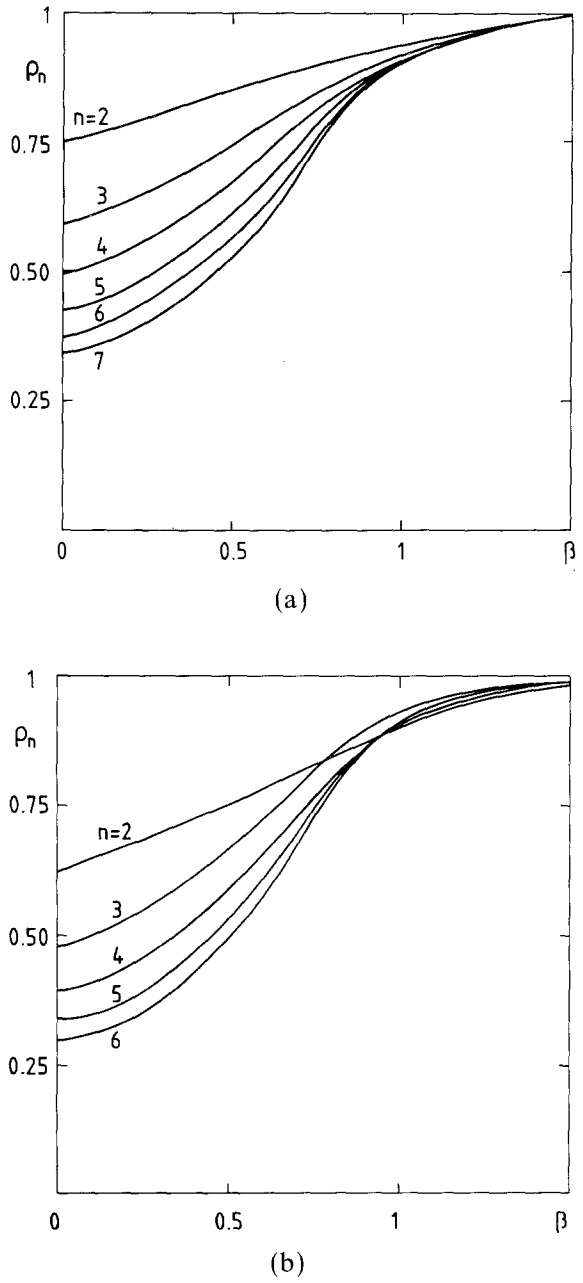

Fig. 2. Plot of the density of a very long polymer ρ_n versus β for different strip widths. (a) Strips in normal direction, (b) strips in diagonal direction.

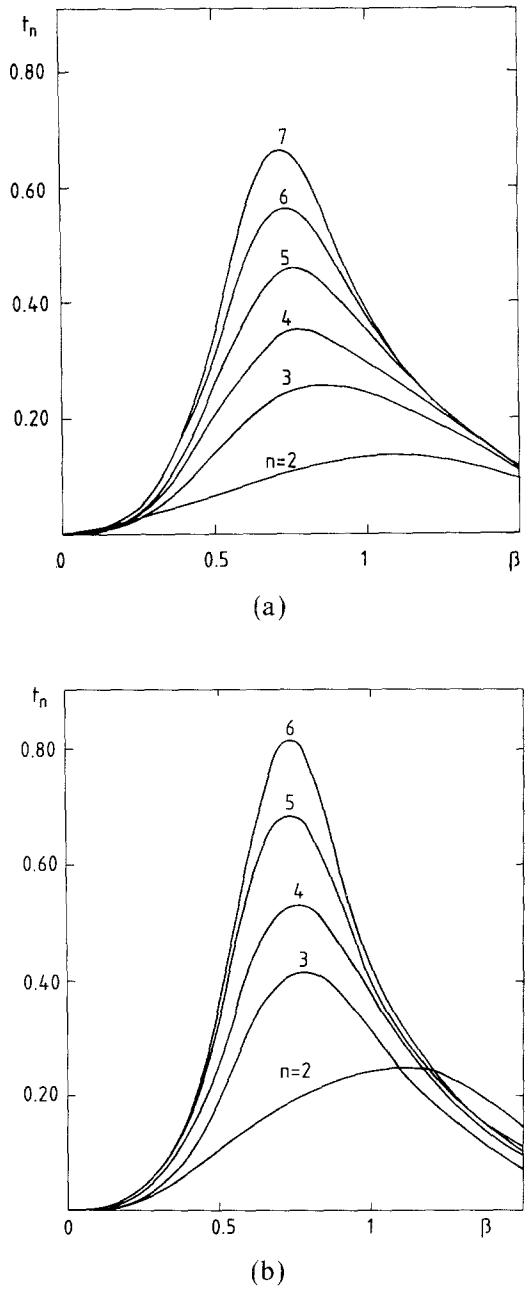

Fig. 3. Coefficient of thermal expansion t_n versus β for different strip widths. (a) Strips in normal direction, (b) strips in diagonal direction.

for increasing n. In formula (20) we compared the sizes n and $n+2$ because of parity effects. Successive approximations of the critical line obtained in this way are given in Fig. 4 for the case of normal strips (very similar results were obtained for diagonal strips). One can see the general good convergence of the results, particularly at low temperatures. The two extremities ($\beta \mapsto 0$ and $\beta \mapsto \infty$) of this critical line are known.

For $\beta = 0$ ($T = \infty$) one has[25] $x^c = 1/\mu_{SQ} = 0.3790528 \pm 0.0000025$, where μ_{SQ} is the connectivity constant of the square lattice while for $\beta \mapsto \infty$ ($T \mapsto 0$), the infinite polymer must cover all the lattice and the equation of the critical line in this region is

$$x^c(T) \simeq \frac{e^{-\beta}}{\mu_{SQ}^{(H)}} \qquad (\beta \mapsto \infty) \tag{21}$$

where $\mu_{SQ}^{(H)}$ is the connective constant of Hamiltonian walks (i.e., SAWs which must visit all the sites) on the square lattice[26] $\mu_{SQ}^{(H)} = 1.4725 \pm 0.0005$. In a similar way we can get estimates of ν by

$$1 + \frac{1}{\nu_n} = \log\left[\frac{d\xi_{n+2}(\tilde{x}_n^c, T)/dx}{d\xi_n(\tilde{x}_n^c, T)/dx}\right] \Big/ \log\left(\frac{n+2}{n}\right) \tag{22}$$

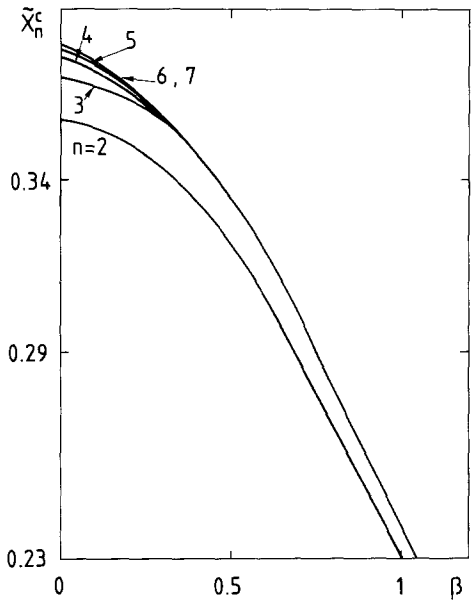

Fig. 4. Plot of the values $\tilde{x}_c^n$ obtained by a two strip renormalization with sizes n and $n+2$ (formula 20). The strips are oriented in normal direction. The convergence is particularly rapid at low temperatures (high β).

We have represented the successive values of the exponent ν obtained in this way for different sizes n versus the inverse temperature $\beta = T^{-1}$ in Fig. 5. As one can see, these exponents in the hightemperature region are more and more constant, tending to the value $\nu_{SAW} = \frac{3}{4}$. Similarly in the lowtemperature region they tend to the collapsed value $\nu = \frac{1}{2}$. When n grows, the variation of ν becomes more and more rapid and concentrated in a small region around $\beta \sim 0.7$. As in the case of animals,[18] these curves intersect almost at the same point for normal strips. Because of parity effects, which are more marked in this case, the curves for diagonal strips intersect at points which are different but rather close. These intersections suggest a value of ν_t around 0.55.

The ratio $n/\pi\xi_n$ at $x^c(T)$ gives—by conformal invariance arguments[27]—the exponent $\eta = 2 - \gamma/\nu$. However, this method for determining γ, which worked rather well in the case of SAWs,[28] does not give conclusive results here, the estimates converging very slowly with increasing size. We do not present these results here.

As in the case of branched polymers,[18] one can give a physical meaning to all the (β, x) plane of Fig. 4. We consider a polymer which spans

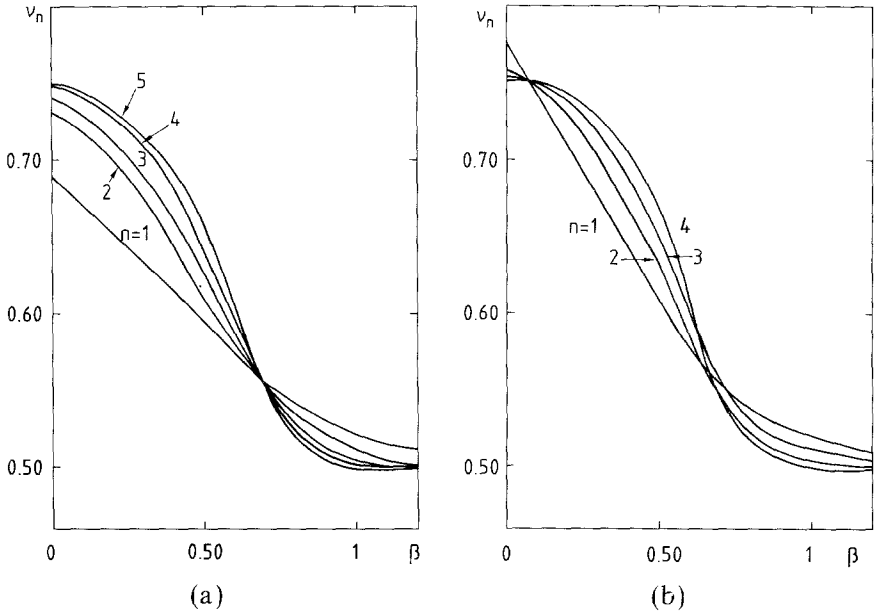

Fig. 5. Plot of the exponent ν_n obtained by a two-strip renormalization with sizes n and $n+2$ (formula 22). When n increases, this exponent converges to the SAW value $\nu = \frac{3}{4}$ for high temperatures (low β) and to the collapsed value $\nu = \frac{1}{2}$ for low temperatures (high β). The curves cross around the value $\nu = 0.55$. (a) Strips in normal direction, (b) strips in diagonal direction.

from column 0 to the column L of the strip at a temperature T. The length of the polymer can fluctuate and is controlled by the fugacity x. It is easy to show[18] that the grand canonical potential of this problem is, for L large

$$\psi = -TL \log \lambda(x, T) \tag{23}$$

and the pressure is given by

$$p = \frac{T}{n} \log \lambda(x, T) \tag{24}$$

A point in the (β, x) plane corresponds thus to the situation where an infinite polymer spans through the strip at a temperature $T = \beta^{-1}$ and a pressure p given by (24). The density of this polymer is[18]

$$\rho = \frac{1}{n} \frac{\partial \log \lambda}{\partial \log x} \tag{25}$$

and its free energy per monomer is[18]

$$f = T\left[\log x - \left(\frac{\partial \log \lambda}{\partial \log x}\right)^{-1} \log \lambda\right] \tag{26}$$

In this picture the critical line corresponds to the isobar $p = 0$. The region $x > x^c(T)$ corresponds to a positive pressure while the region $x < x^c(T)$ corresponds to a negative pressure, i.e., to a force that swells the polymer. By crossing the isobar $p = 0$ in the high-temperature region one has a second-order phase transition while the crossing in the low-temperature region gives rise to a first-order phase transition with a jump of the density ρ (25). This can be seen on Fig. 6 where we have represented the densities ρ versus x for several values of the temperature. We note that because of formula (25) the jump of density in the low-temperature phase must coincide with the point where the correlation length (12) diverges (i.e., with point $p = 0$). A similar effect is observed for branched polymers.[18]

We should note here that, because for $T < \theta$ the transition $x \mapsto x^c(T)$ is a first-order transition, the correlation length ξ_n does not have the finite-size scaling form (19) in the low-temperature region but a more complicated one depending in particular on the parity of the strip width n and on the geometry of the strip. The application of eq. (20) in this region of temperatures gives, however, correct estimates of $x^c(T)$ simply because the correlation length of the two-dimensional system diverges at this point. In a similar way the exponent $\frac{1}{2}$ obtained in this region can be considered as the exponent of a discontinuity fixed point.[29] With the introduction of the fugacity x, the θ point which was shown in Section 2 to be a point of

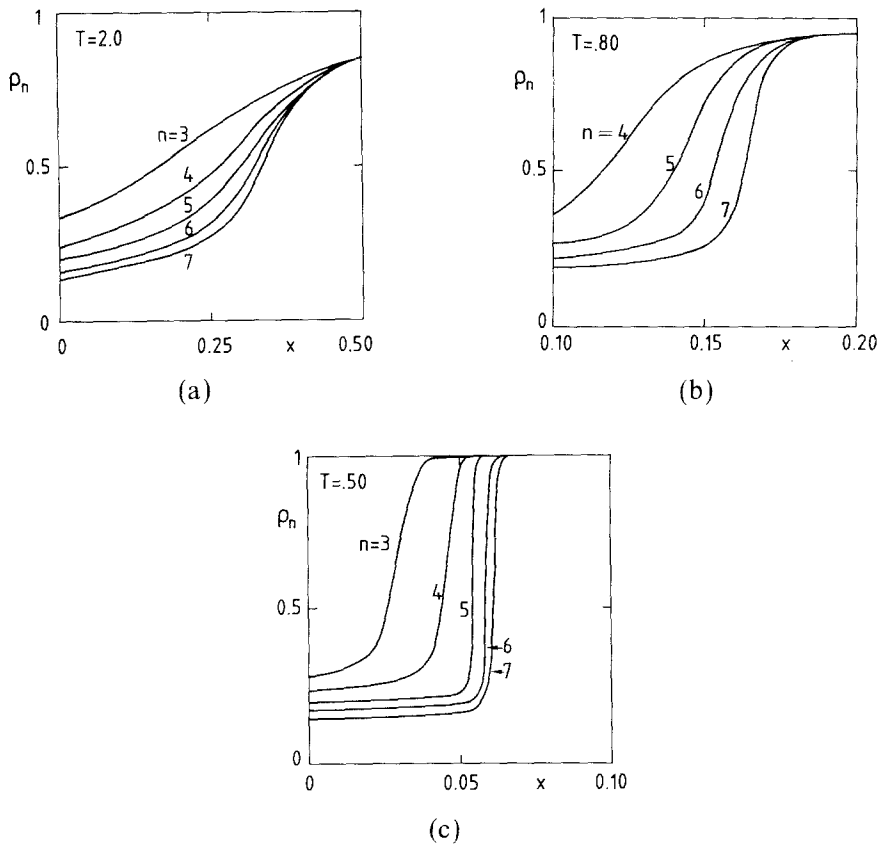

Fig. 6. Variation with x of the density ρ (25) at different temperatures and for different strip widths. This variation is continuous at high temperatures while the curves at low temperatures indicate a discontinuity for $n \to \infty$. The strips are taken in normal direction.

second-order phase transition for a very long polymer can also be considered in the (β, x) plane as the end point of a line of second-order phase transitions, i.e., as a tricritical point. We determine the characteristics of this tricritical point in the following section.

4. DETERMINATION OF THE θ POINT AND ITS TRICRITICAL EXPONENTS

For a complete description of the tricritical point[30] we must determine the temperature θ and calculate the values of three independent exponents. We have already introduced the exponents ν_t and γ_t which describe the geometrical properties of a very long polymer at the θ point.

In the following we also calculate the exponent ν_u, which is the exponent of a thermal length (persistance length[18,30,31]). This represents the correlations of thermal fluctuations and diverges like $|T-\theta|^{-\nu_u}$. All other exponents can be obtained using these three exponents and the scaling laws.[30]

In the case of animals[18] or of the tricritical Ising model,[31] these exponents were calculated by rather sophisticated techniques using three size renormalizations or renormalizations with two correlation lengths. These methods did not work here because of the parity effects and because the results converged slowly with increasing size. We have obtained better results by considering the finite-size scaling form of the geometrical quantities.

We first consider the density ρ_n (17). In the neighborhood of temperature θ one expects the finite-size scaling form (valid for $n \gg 1$ and $T-\theta \ll 1$)

$$\rho_n(T) \sim n^{(1/\nu_t)-2} F_\rho[(T-\theta)\, n^{1/\nu_u}] \tag{27}$$

We have thus calculated the quantities

$$[X_n(T)]^{-1} = \frac{\log[\rho_{n+2}(T)/\rho_n(T)]}{\log[n+2/n]} + 2 \tag{28}$$

which are plotted versus $\beta = T^{-1}$ in Fig. 7. Because of formula (27) one expects that the curves for different n will cross at $\beta^c = \theta^{-1}$ and that the values of X_n at the intersection will give ν_t. As can be seen on Fig. 7(a),

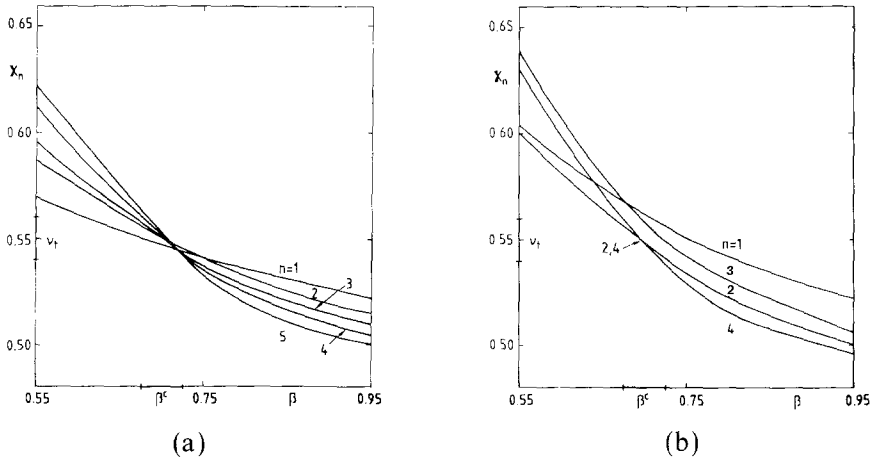

Fig. 7. Plot of X_n (28) versus β. For large n the curves should intersect at $(\beta_t \cdot \nu_t)$. Our estimate is indicated with its error bars (See formula 29). (a) Strips in normal direction, (b) strips in diagonal direction.

these curves cross rather well in the case of normal strips. From this figure we deduce the estimates

$$(\beta^c)^{-1} = \theta = 1.42 \pm 0.04 \qquad \text{and} \qquad \nu_t = 0.55 \pm 0.01 \tag{29}$$

The curves for diagonal strips don't cross so well (Fig. 7b) because of the parity effects. There is an intersection 1–3 for n odd and an intersection 2–4 for n even. It is difficult to extrapolate these results with only one point for each parity. We note however that the two intersections are rather close to (29), the intersection 2–4 for the largest sizes being in good agreement with $\nu_t = 0.55$. We have also done similar calculations in the case of the triangular or hexagonal lattices. The parity effects were also marked in these cases but the results were compatible with (29). We note here that because of formulas (12) and (17) the quantities $X_n(T)$ of formula (28) are very similar to the $\nu_n(T)$ of eq. (22). The curves of Fig. 5 crossed also at values compatible with (29).

We now consider the coefficient of thermal expansion t_n (18). Its finite-size scaling form is

$$t_n(T) \sim n^{1/\nu_u} F_t[(T-\theta)\, n^{1/\nu_u}] \tag{30}$$

for $n \gg 1$ and $T - \theta \ll 1$. The quantity Y_n defined by

$$[Y_n(T)]^{-1} = \frac{\log[t_{n+2}(T)/t_n(T)]}{\log[n+2/n]} \tag{31}$$

varies slowly with the temperature T, and the curves representing Y_n do not cross very well. For getting an estimate of ν_u we have thus preferred the following method. We have calculated the $Y_n(\theta)$ for various sizes n in the case of the square lattice with the two strip directions, the hexagonal and the triangular lattices (the θ points for these two lattices were evaluated in a way similar to formula 29). We have plotted these Y_n versus n^{-1} in Fig. 8, a choice which gave rather smooth curves for all the data. The variation of Y_n due to the error bars in the determination of θ is smaller than the size of the points in this figure. From this figure we deduce

$$\nu_u = 1.15 \pm 0.15 \tag{32a}$$

From the values of ν_u and ν_t (29) one can get the exponent α of the specific heat by the relation $2 - \alpha = \nu_u/\nu_t$ (see Ref. 18)

$$\alpha = -0.1 + 0.1 \tag{32b}$$

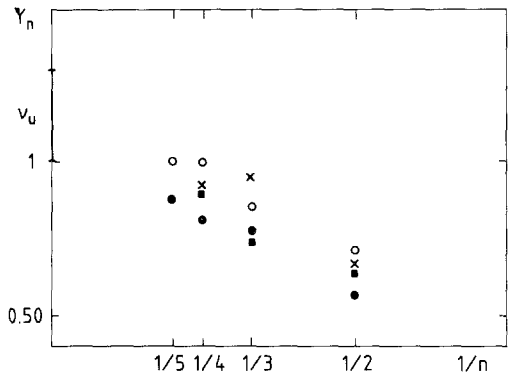

Fig. 8. Plot of the quantities $Y_n(\theta)$ (31) versus n^{-1}. ●, Square lattice and strips in normal direction, ×, square lattice and strips in diagonal direction, ○, hexagonal lattice, ■, triangular lattice. The final estimate of v_u is indicated with its error bars (see formula 32).

Our central value is negative, suggesting that the specific heat does not diverge at the θ point. This explains the smooth maxima observed in Fig. 1. From v_u (32a) and v_t (29) we deduce also the value of the cross-over exponent

$$\phi_t = \frac{v_t}{v_u} = 0.48 \pm 0.07 \tag{33}$$

We finally consider the generating functions defined in (10)

$$G(x, T) = \sum_{\vec{R}} \sum_{l,b} x^l e^{\beta b} w_{o\vec{R}}(l, b) \tag{34}$$

We have shown[28] how such functions can be calculated by using a transfer matrix technique in the case of SAWs. It is easy to generalize this method to the case of interacting polymers. As was remarked[28] the function $G(x, T)$ depends on polymers of every length. However, its asymptotic behavior (11) when $x \mapsto x^c(T)$ depends on very long polymers only. On a strip one calculates a function $G_n(x, T)$. When $x \mapsto x_n^c(T)$, G_n behaves as

$$G_n(x, T) \sim \frac{R_n(T)}{1 - \lambda(x, T)} \tag{35}$$

and it diverges for $x = x_n^c(T)$. The residue $R_n(T)$ depends only on the very long polymers on the strip and the results obtained by considering R_n con-

verge more rapidly with increasing n than the results obtained with G_n. The finite-size scaling form of R_n is[28]

$$R_n(T) \sim n^{(\gamma_t/\nu_t)^{-1}} F_R[(T-\theta)\, n^{1/\nu_u}] \tag{36}$$

for $n \gg 1$ and $T-\theta \ll 1$. We have thus calculated the quantities

$$Z_n(T) = \frac{\log[R_{n+2}(T)/R_n(T)]}{\log[n+2/n]} + 1 \tag{37}$$

which are plotted versus $\beta = T^{-1}$ in Fig. 9 in the case of normal strips. On this figure one can observe several crossings. These crossings are in the neighborhood of the critical temperature θ (29). It is, however, clear from this figure that the results have not yet completely converged. (We have been limited to the strip width $n=6$ here since the size of the transfer matrix for calculating R_n grows more rapidly than for calculating the correlation lengths[28]). A reasonable estimate is

$$\gamma_t/\nu_t = 1.80 \pm 0.05 \tag{38}$$

Using (29) one has also

$$\gamma_t = 1 \pm 0.05 \tag{39}$$

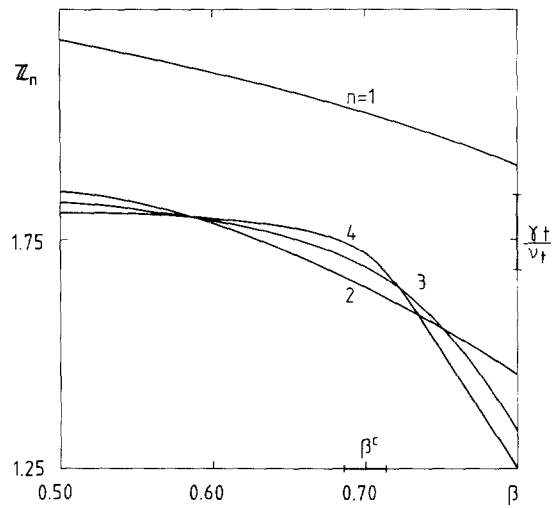

Fig. 9. Plot of Z_n (37) versus β for different widths n in the case of normal strips. We have indicated our estimate γ_t/ν_t with its error bars (see formula 38).

5. CONCLUSION

Using the transfer matrix technique we have thus determined the properties of a lattice model with two parameters, the temperature $T=\beta^{-1}$ and the fugacity x. We have shown the existence of a θ point where the thermal and geometrical properties of a very long polymer display a singularity. This point can also be considered as a tricritical point in the (T, x) plane and we have determined the exponents of this point using finite-size scaling. It would also be of interest to calculate the properties of a system with several polymers. This could be done by introducing another fugacity y conjugated to the number of polymers and by generalizing the transfer matrix technique for several polymers already introduced in Ref. [28] in the case of non-interacting, self-avoiding walks. We plan to do such a calculation in the future.

We now compare our results with those which have already been proposed in the literature. The tricritical exponents for a magnetic spin system with s component spin variables have been calculated to lowest order in $\varepsilon'=3-D$[32] with the results for the polymer problem ($s=0$) in two dimensions ($\varepsilon'=1$)

$$\nu_t = 0.5055 \tag{40a}$$

$$\nu_u = \nu_t/\phi_t = 0.7944 \tag{40b}$$

$$\frac{\gamma_t}{\nu_t} = 2-\eta_t = 1.9986 \tag{40c}$$

(The results 40a and 40c are given to the second order in ε' and the result 40b to the first order). These exponents (40) have also been recently recovered in a direct polymer approach.[14] The results of formulas (40) don't agree well with our transfer matrix calculation. This is not surprising since there is a similar difference between the results of the asymptotic ε' expansion for the two-dimensional tricritical Ising model ($s=1$) exponents and the value of these exponents which are now considered to be exact.[30] The values (40) were initially found in agreement with Monte Carlo calculations[17], but we think that the results of these calculations are difficult to interprete because the algorithms used do not sample in an efficient way the compact configurations which are the most important in the low-temperature phase. Moreover, in Monte Carlo simulations one works with rather short chains and some surface or extremity effects might be present (surface effects have already been observed in Monte Carlo simulations for branched polymers[33]).

Exponents ν_u and η_t have later been calculated to the next order[34] giving

$$\nu_u = \nu_t/\phi_t = -1.0339 \tag{41a}$$

$$\frac{\gamma_t}{\nu_t} = 2 - \eta_t = 1.980 \tag{41b}$$

However, the correction to ν_u is now too important since this exponent becomes negative (a similar effect is observed for the tricritical Ising model with $s = 1$[34]). We think that the way the ε' series behaves is not completely understood in this case, so it is difficult to extract information from the ε' expansion at $D = 2$. A recent conjecture[35] identifies the $2D$ linear polymers at the θ point with the indefinitely growing self-avoiding walks[36] and predicts the values

$$\nu_t = 0.567 \pm 0.003 \tag{42a}$$

$$\gamma_t = 1 \text{ (exact)} \tag{42b}$$

The value (42b) is in agreement with our result (39). The value (42a) seems slightly too high when compared to (29), but we think that the precision of the results (42a) and (29) is not sufficient to rule out this conjecture. The exponent ν_t has also been related to the exponents of other kinetic walks,[37] but these predictions don't agree well with our result. Finally, experiments on $2D$ polymer monolayers[15] gave a value $\nu_t = 0.56 \pm 0.01$, which is in agreement with our calculation.

In conclusion, we would like to mention that the collapsed phase of our model has some features which are reminiscent from frustrated systems such as a very strong dependence on boundary conditions or a nonnull entropy at zero temperature. This suggests that the collapse transition could perhaps be interpreted as a spin-glass phase transition. We hope to sharpen this analogy in the future.

ACKNOWLEDGMENTS

We thank B. Derrida for many useful discussions, B. Duplantier for a careful reading of the maniscript, and B. Nienhuis for a correspondence on this subject.

REFERENCES

1. P. J. Flory, *Principles of Polymer Chemistry* (Cornell University Press, New York, 1966).
2. P. G. de Gennes, *Scaling Concepts in Polymer Physics* (Cornell University Press, New York, 1979).

3. J. Des Cloizeaux and G. Jannink, *Polymères en Solution, leur modélisation et leur Structure* (Editions de Physique, to appear).
4. I. Nishio, S. T. Sun, G. Swislow, and T. Tanaka, *Nature* **281**:208 (1979).
5. D. C. Rapaport, *Phys. Lett. A* **48**:339 (1974); D. C. Rapaport, *J. Phys. A* **10**:637 (1977).
6. I. Webman, J. L. Lebowitz, and M. H. Kalos, *Macromolecules* **14**:1495 (1981).
7. C. Domb, *Polymer* **15**:259 (1974).
8. M. A. Moore, *J. Phys. A* **10**:305 (1977).
9. A. R. Massih and M. A. Moore, *J. Phys. A* **8**:237 (1975).
10. I. M. Lifschitz, A. Y. Grassberg, and A. R. Khokhlov, *Rev. Mod. Phys.* **50**:683 (1978).
11. P. G. de Gennes, *J. Phys. Lett.* **36**:L55 (1975).
12. K. Kremer, A. Baumgartner, and K. Binder, *J. Phys. A* **15**:2879 (1982).
13. B. Duplantier, *J. Phys.* **43**:991 (1982).
14. B. Duplantier, Preprint Saclay SPhT 85/153.
15. R. Villanove and S. Rondelez, *Phys. Rev. Lett.* **45**:1502 (1980).
16. J. Tobochnik, I. Webman, J. L. Lebowitz, and M. H. Kalos, *Macromolecules.* **15**:549 (1982).
17. A. Baumgartner, *J. Phys.* **43**:1407 (1982).
18. B. Derrida, H. J. Herrmann, *J. Phys.* **44**:1365 (1983).
19. B. Derrida and H. Saleur, *J. Phys. A* **18**:L1075 (1985).
20. B. Nienhuis, *Phys. Rev. Lett.* **49**:1062 (1982).
21. G. Sarma, in *Ill Condensed Matter*, 1978, eds. R. Balian, R. Maynard, and G. Toulouse (Les Houches, North Holland, 1978).
22. D. J. Klein, *J. Stat. Phys.* **23**:561 (1980).
23. B. Derrida, *J. Phys. A* **14**:L5 (1981).
24. M. N. Barber, in *Phase Transitions and Critical Phenomena*, vol. 8, C. Domb and J. L. Lebowitz, eds. (1983).
25. I. G. Euting and A. J. Guttman, *J. Phys. A* **18**:1007 (1985).
26. T. G. Schmalz, G. E. Hite, and D. J. Klein, *J. Phys. A* **17**:445 (1984); H. Orland, C. Itzykson, and C. Dominicus, *J. Phys. Lett.* **46**:L355 (1985).
27. J. L. Cardy, *J. Phys. A* **17**:L385 (1984).
28. H. Saleur and B. Derrida, *J. Stat. Phys.* **44**:225 (1986).
29. B. Nienhuis and M. Nauenberg, *Phys. Rev. Lett.* **35**:477 (1978).
30. I. D. Lewine and S. Sarbach, in *Phase Transitions and Critical Phenomena*, vol. 9, C. Domb and J. L. Lebowitz, eds. (1985).
31. P. A. Rikvold, W. Kinzel, J. D. Gunton, and K. Kashi, *Phys. Rev. B* **28**:2686 (1983); P. D. Beale, *J. Phys. A* **17**:L33 (1984); H. J. Herrmann, *Phys. Lett. A* **100**:256 (1984).
32. M. J. Stephen and J. L. McCauley, *Phys. Lett. A* **44**:89 (1973).
33. R. Dickman and W. C. Schieve, *J. Phys.* **45**:1727 (1984).
34. A. L. Lewis and F. W. Adams, *Phys. Rev. B* **18**:5103 (1978).
35. A. Coniglio, N. Jan, I. Majid, and H. E. Stanley, Preprint 1985.
36. K. Kremer and J. W. Lyklema, *J. Phys. A* **18**:1511 (1985).
37. J. W. Lyklema, *J. Phys. A* **18**:L625 (1985).